PAPER

Laser irradiation-induced laminated graphene/MoS_2 composites with synergistically improved tribological properties

To cite this article: Ting Luo *et al* 2018 *Nanotechnology* **29** 265704

Nanotechnology 29 (2018) 265704 (11pp) https://doi.org/10.1088/1361-6528/aabcf5

Laser irradiation-induced laminated graphene/MoS_2 composites with synergistically improved tribological properties

Ting Luo[1], Xinchun Chen[2], Peisheng Li[3], Ping Wang[1], Cuncheng Li[1], Bingqiang Cao[1,4,5], Jianbin Luo[2] and Shikuan Yang[3,5]

[1] Materials Research Center for Energy and Photoelectrochemical Conversion, School of Material Science and Engineering, University of Jinan, Jinan 250022, Shandong, People's Republic of China
[2] State Key Laboratory of Tribology, Department of Mechanical Engineering, Tsinghua University, Beijing 100084, People's Republic of China
[3] Institute for Composites Science Innovation, School of Materials Science and Engineering, Zhejiang University, Hangzhou 310027, People's Republic of China
[4] Department of Physics and Institute of Laser, Qufu Normal University, Qufu 273165, Shandong, People's Republic of China

E-mail: mse_caobq@ujn.edu.cn and shkyang@zju.edu.cn

Received 9 January 2018, revised 2 March 2018
Accepted for publication 10 April 2018
Published 2 May 2018

Abstract

Engineering lubricant additives that have extraordinary friction reduction and anti-wear performance is critical to almost any modern mechanical machines. Here, we demonstrate the fabrication of laminated lubricant additives that can combine the advantages of zero-dimensional nanospheres and two-dimensional nanosheets. A simple *in situ* laser irradiation method is developed to prepare the laminated composite structure composed of ideally ultrasmooth MoS_2 sub-microspheres embedded within multiple layers of graphene. These ultrasmooth MoS_2 spheres within the laminated structure can change sliding friction into rolling friction under strong shear force created by moving contact surfaces to significantly reduce the friction. Meantime, the graphene layers can behave as 'protection pads' to efficiently avoid the formation of scars on the metal-to-metal contact surfaces. Overall, the laminated composites as lubricant additives synergistically improve the friction reduction and anti-wear properties. Additionally, due to the unique loosely packed laminated structure, the composites can stably disperse in the lubricant for more than 15 d and work under high temperatures without being oxidized. Such constructed laminated composites with outstanding tribological properties by an *in situ* laser irradiation method supply a new concept in designing lubricant additives that can combine the advantages of 0D and 2D structures.

Supplementary material for this article is available online

Keywords: 0D/2D laminated structure, laser irradiation, lubricant additives, tribological property

(Some figures may appear in colour only in the online journal)

1. Introduction

Friction is ubiquitous in nature, which wasted nearly 1/3 of human beings' consumed energy every year [1]. Therefore, reducing friction is critical to save energy and alleviate

[5] Author to whom any correspondence should be addressed.

environmental pollution induced by the fossil energy consumption. Various approaches have been developed to minimize friction [2–4]. Among them, applying lubricants between contacting surfaces is probably one of the most successful strategies [5–7]. Recently, introducing micro/nanoscale additives into the lubricants has been proven to be able to further improve their friction reduction performance [8–12]. Excellent lubricant additives should have appropriate size, morphology, structure, and stiffness, as well as high stability and good dispersity in the lubricants. On one hand, zero-dimensional (0D) spherical particles can roll between contacting surfaces to reduce friction when used as lubricant additives [9–12]. On the other hand, two-dimensional (2D) layered materials as lubricant additives can behave as 'protection pads' between contacting surfaces to significantly enhance the anti-wear performance of the lubricant [13–15]. Therefore, 0D/2D composite structures may generate lubricant additives with outstanding tribological (i.e., friction reduction and anti-wear) performance. However, what is the favored organization way of the 0D and 2D structures to achieve the best tribological performance and how to experimentally realize it are still elusive [5].

On one hand, graphite and molybdenum disulfide (MoS_2), as two typical layered materials, have been widely studied as effective surface lubricants due to weak interatomic interactions and low strength shearing between interlayers [6, 16, 17]. The dispersion of pristine graphene and MoS_2 nanosheets in lubricating oil is usually unstable due to their high specific surface area. Serious aggregation and precipitation of graphene and MoS_2 nanosheets will result in unstable tribological performance [5, 7, 18–20]. On the other hand, MoS_2 spheres exhibit improved tribological behavior compared to the micro/nanoscale slices due to the better chemical stability and the spherical shape [8, 10, 11, 20]. However, fabrication of MoS_2 spheres requires high temperature (usually > 900 °C), high purity expensive and sometimes toxic gas precursors (H_2S/H_2), and harsh experimental conditions, which makes it unrealistic to employ MoS_2 spheres as lubricant additives [8, 21].

Here, we demonstrate a simple and one-step laser irradiation method to construct laminated composite structures formed by ultrasmooth and perfectly MoS_2 sub-microspheres wrapped within multiple layers of reduced graphene oxide (L-rGO/MoS_2), which can effectively combine the advantages of 0D and 2D structures when used as lubricant additives (figure 1). These perfectly spherical MoS_2 particles can substantially transform sliding friction into rolling friction between two neighboring graphene layers acting as the 'protection pads' to simultaneously reduce the friction and enhance the anti-wear properties, effectively combining the advantages of 0D and 2D structures as lubricant additives. Importantly, the L-rGO/MoS_2 structure can be well-dispersed in the lubricating oil without showing obvious precipitants for 15 d. Moreover, such composites can work under high temperatures without being oxidized. Therefore, the L-rGO/MoS_2 structure can synergistically improve the tribological performance of the lubricating oil as lubricant additives. A simple one-step method is developed to prepare the L-rGO/MoS_2 composite structures by laser irradiation of a dispersion composed of graphene oxide (GO) and MoS_2 nanoflakes. The MoS_2 nanoflakes are reshaped into ultrasmooth spheres and simultaneously are wrapped within the adjacent graphene nanosheets produced by laser-reduction of GO under the high temperature created by the laser irradiation. To the best of our knowledge, this is the first report of one-step fabrication of L-rGO/MoS_2 composite structures that can integrate the advantages of 0D and 2D materials when used as lubricant additives, which opens up a new avenue towards engineering high-performance lubricant additives.

2. Experimental section

2.1. Preparation of the L-rGO/MoS_2 composite structure

MoS_2 nanoflakes were synthesized by a hydrothermal method. Typically, 0.5 g sodium molybdate dehydrate (99.0% purity, Aladdin) and 0.8 g thioacetamide (99.0% purity, Aladdin) were added into 50 ml deionized water. After being stirred for 30 min, the solution was transferred into a 100 ml Teflon-lined stainless steel autoclave and heated at 200 °C for 24 h. Then, the autoclave was cooled instantly to room temperature by a cold water bath. The MoS_2 flakes (figure S1(a) is available online at stacks.iop.org/NANO/29/265704/mmedia) were collected by centrifugation and washed several times with deionized water. GO nanosheets (figure S2(a)) were prepared by exfoliation of graphite (99.8% purity, 325 mesh, Alfa Aesar) according to a modified Hummers method [22].

The L-rGO/MoS_2 composite structure was fabricated by pulse laser irradiation of a water dispersion of GO and MoS_2 at ambient conditions. 100 mg of the above-prepared MoS_2 flakes was added into 15 ml of a homogeneous GO dispersion (1.5 mg ml^{-1}) (referred as GO/MoS_2), followed by stirring for 30 min to form a colloidal solution. A KrF excimer laser (10 Hz, 25 ns, Coherent, CompexPro 205) with a wavelength of 248 nm was used as the light source. The laser beam was focused into an area of around 0.87 cm^2 (1.1 cm × 0.79 cm) at the solution through a convex lens with a focal length of 150 mm. The laser irradiation of the GO/MoS_2 dispersion was lasted for different times at an energy fluence of 400 mJ $pulse^{-1}$ cm^{-1}. The GO/MoS_2 dispersion was continuously magnetically stirred during laser irradiation to make sure uniform irradiation and prevent sedimentation formation. After laser irradiation, the 0D/2D L-rGO/MoS_2 particles were frozen dried to obtain powder products for further characterizations. Reduced graphene oxide (rGO) nanosheets and MoS_2 spherical sub-microspheres were obtained by laser irradiation of dispersions of pure GO and MoS_2 nanoflakes, respectively (figures S1(b) and S2(b)).

2.2. Material characterizations

The morphology of different samples was observed with a scanning electron microscope (SEM, FEI Quanta 250 FEG). The x-ray diffraction (XRD) pattern was obtained with an XRD apparatus (D8-Advance, Bruker) operated at 40 kV and 40 mA using the Cu-Kα line ($\lambda = 0.154\,184$ nm) as the

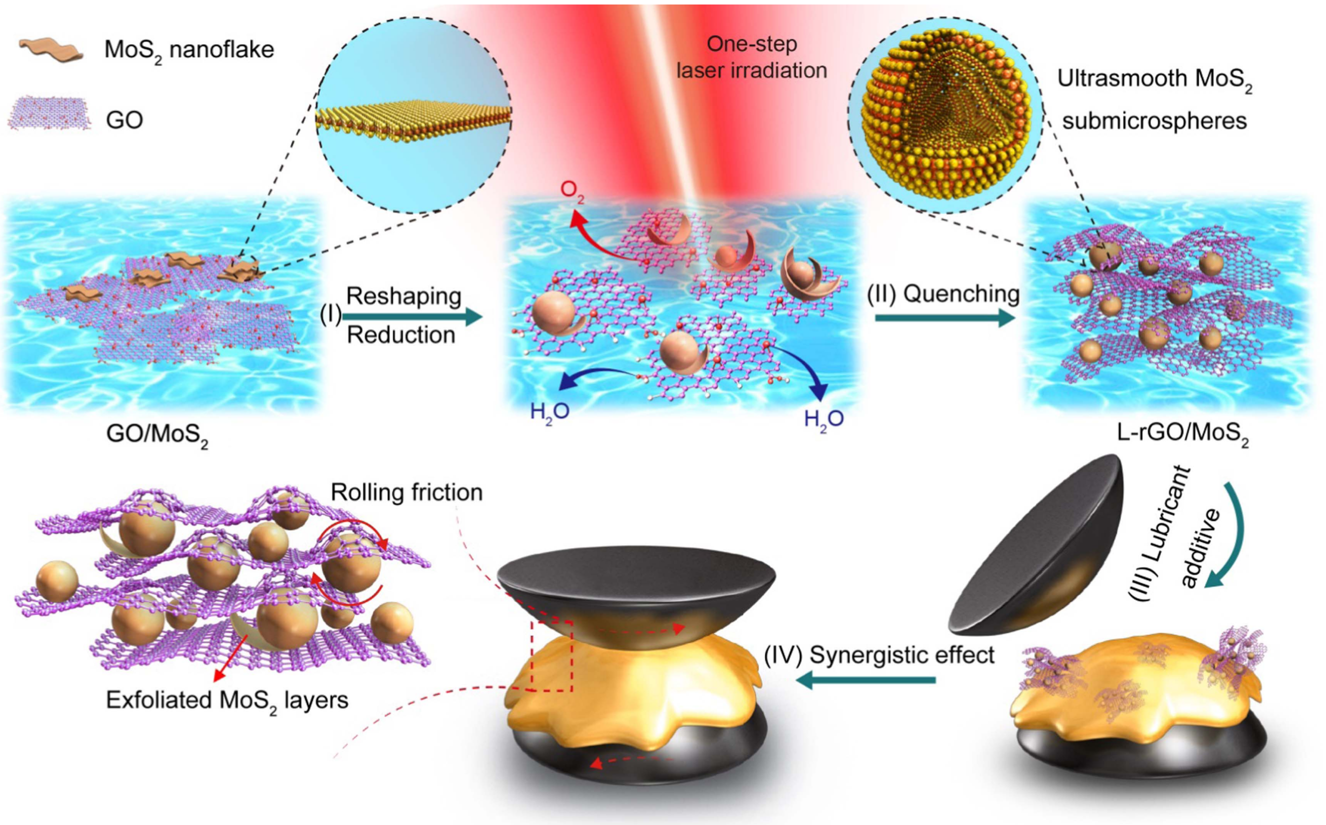

Figure 1. Schematic of the formation process of the L-rGO/MoS_2 composite structures and the working mechanism of friction reduction and anti-wear when they are used as lubricant additives. Process I. Pulsed laser irradiation of GO/MoS_2 creates localized high temperature and pressure, which induce reshaping of MoS_2 and reduction of GO to rGO. Process II. The quenching process of the surrounding liquid medium 'freezes' and solidifies the liquid MoS_2 droplet into ideally spherical particles. Several graphene layers wrap a tremendous amount of MoS_2 spheres, giving rise to the formation of L-rGO/MoS_2 composite structure. Process III. The L-rGO/MoS_2 composite structures are introduced into engine oil as lubricant additives. Process IV. The unique L-rGO/MoS_2 composite structure can combine the advantages of quasi-fullerene-like MoS_2 spheres and graphene nanosheets regarding friction reduction and anti-wear.

excitation source. Microstructural examination was characterized with a transmission electron microscope (TEM, JEM-2100F) under a 200 kV acceleration voltage. Raman spectrometer equipped with a 532 nm laser (LabRAM HR Evolution, HORIBA) was used for recording the Raman scattering spectra of different samples. The UV–visible absorption spectra were measured with a Shimadzu UV-3600 spectrophotometer (Shimadzu). The morphology of wear surface after four-ball test was observed with a laser scanning confocal microscope (LSCM, KEYENCE Corporation, VK-X250K). The binding energies of Mo in different samples were detected by x-ray photoelectron spectroscopy (XPS, Thermo Fisher, with an Al Kα x-ray source).

2.3. Evaluation of the tribological properties

A four-ball tribology tester (MM-W1B, Shijin-Jinan, China) was used to study the tribological properties. The tester was operated with one steel ball under load *f* rotating at a speed of ω against three steel balls held stationary in the form of a cradle

which is controlled by a DC servo motor. The steel balls with a hardness of 64-66 HRC were selected according to the National Standard of China (G20, GB/T308-2002). The 10w-40 engine oil was used as a reference lubricant in the tribology test. The kinematic viscosity of the reference oil is 122 $mm^2\ s^{-1}$ at 40 °C. Lubricant additives were added into the base oil at a concentration of 0.2 wt%, which were generally ultrasonically agitated for 30 min. Due to the poor dispersity, the GO/MoS_2 hybrids were sonicated for 2 h. The rotation speed of the rolling ball is 1200 rpm under a load of 392 N. The duration time is 30 min. The tests were performed at room temperature unless otherwise specified. Friction reduction was recorded automatically with a computer controlled data acquisition card. Wear scar diameter (WSD) was measured with a metallographic microscope. After washing with petroleum ether and acetone, the size and morphology of the wear scar area were evaluated by SEM and digital stereomicroscope (VHX-5000, KEYENCE).

3. Results and discussion

3.1. Fabrication and characterization of the L-rGO/MoS_2 composites

A simple one-step laser irradiation of a water suspension composed of GO/MoS_2 is used to fabricate the L-rGO/MoS_2 composite structure (figure 1). Due to the ultrahigh pressure

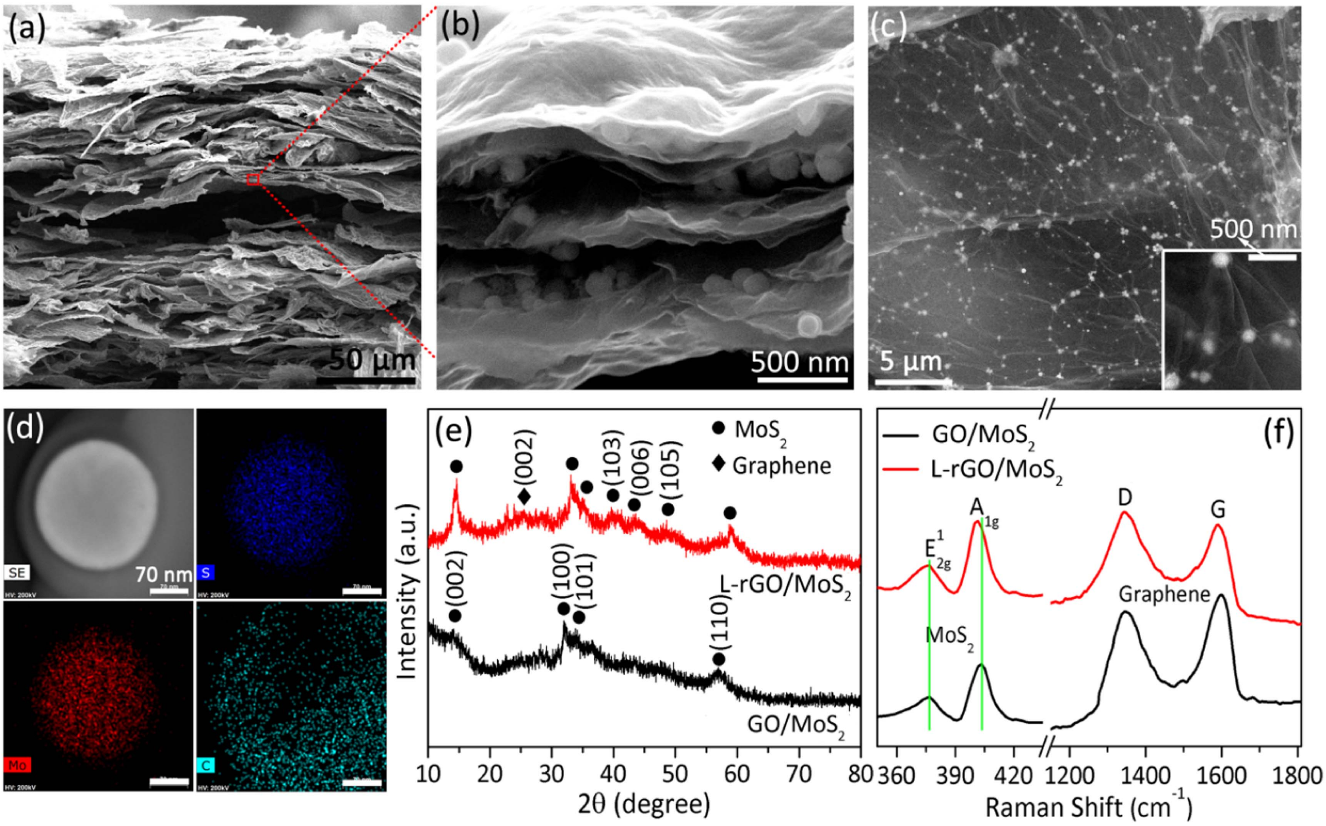

Figure 2. Scanning electron microscopy micrographs of the L-rGO/MoS_2 composite structure from (a), (b) the cross section and (c) the top view. (d) Element mapping of a MoS_2 sphere within the composite structure. (e) XRD results and (f) Raman spectra of raw GO/MoS_2 and L-rGO/MoS_2 composite structure.

(1 GPa) and ultrahigh temperature (10^4 K) around the laser spot-material interface induced by laser irradiation [23–29], MoS_2 nanoflakes are transformed into ideally spheres (figures 1 and S1) and meanwhile GO nanosheets are reduced to rGO with prominently reduced size (figures 1, S2, and S3). Interestingly, MoS_2 spheres are wrapped within graphene layers, forming the L-rGO/MoS_2 composite structure (figures 2(a)–(c)). The number density of MoS_2 spheres on rGO nanosheets is about 7/μm^2 obtained by directly counting from figure 2(c). The energy-dispersive x-ray spectroscopy elemental mapping results indicate that the ultrasmooth MoS_2 sub-microspheres are perfectly wrapped by graphene nanosheets (figure 2(d)), which can effectively prevent the aggregation of rGO nanosheets by forming graphene wrinkles and the pulverization of MoS_2 spheres during the high-load friction process as proved later (figure 1).

Representative XRD patterns of raw GO/MoS_2 hybrids and L-rGO/MoS_2 composites prove the formation of MoS_2 spheres with a hexagonal structure. The broad diffraction peak appearing at ~26.5° in L-rGO/MoS_2 composites can be indexed to the (002) disorderly stacked layer of rGO nanosheets, proving the laser-induced reduction of GO to rGO (figure 2(e)). The Raman spectrum shows that the in-plane E^1_{2g} phonon mode of MoS_2 sphere slightly redshifts compared to that of the nanoflakes, induced by the morphological transition from nanoflakes to quasi-fullerene-like MoS_2 spheres as discussed later (figure 2(f)). The relative peak intensity ratio of I_G/I_D of graphene decreases when compared with that of GO, which is caused by laser-induced distortion and fragmentation of GO (figures S2 and S3).

High-resolution transmission electron microscope characterization indicates that MoS_2 nanoflakes have a poor crystallinity (inset in figure 3(a)). After laser irradiation, MoS_2 nanoflakes are transformed into MoS_2 spheres (figure 3(b)). MoS_2 spheres possess a nearly closed-cage structure due to the partial bonds closing at the edge of spheres (figures 3(c), (d)). Compared with raw MoS_2 flakes, ultrasmooth MoS_2 sub-microspheres show better-resolved lattice fringes with an interplanar distance of 0.62–0.64 nm from the (002) planes. The external layers of the MoS_2 sub-microspheres show a 1.5%–3% dilation of interlayers spacing along the *c* axis. The expansion is generally due to the presence of residual stresses in the curved layers. Some edge dislocations can also be observed within the quasi-fullerene-like structure (see red circle-marked area in figures 3(c), (d)). The subtle redshift of A_{1g} phonon mode in the L-rGO/MoS_2 composites (figure 2(e)) is an indicator of these changes in the microstructure and the morphology. More importantly, MoS_2 spheres are wrapped by the graphene layers, instead of simply attaching on the graphene layers, which can be proved by the bond layer between MoS_2 and graphene (figures 3(d) and S4). Such interfacial bonds can stabilize the sulfide particles on the graphene support, which helps to prevent graphene and MoS_2

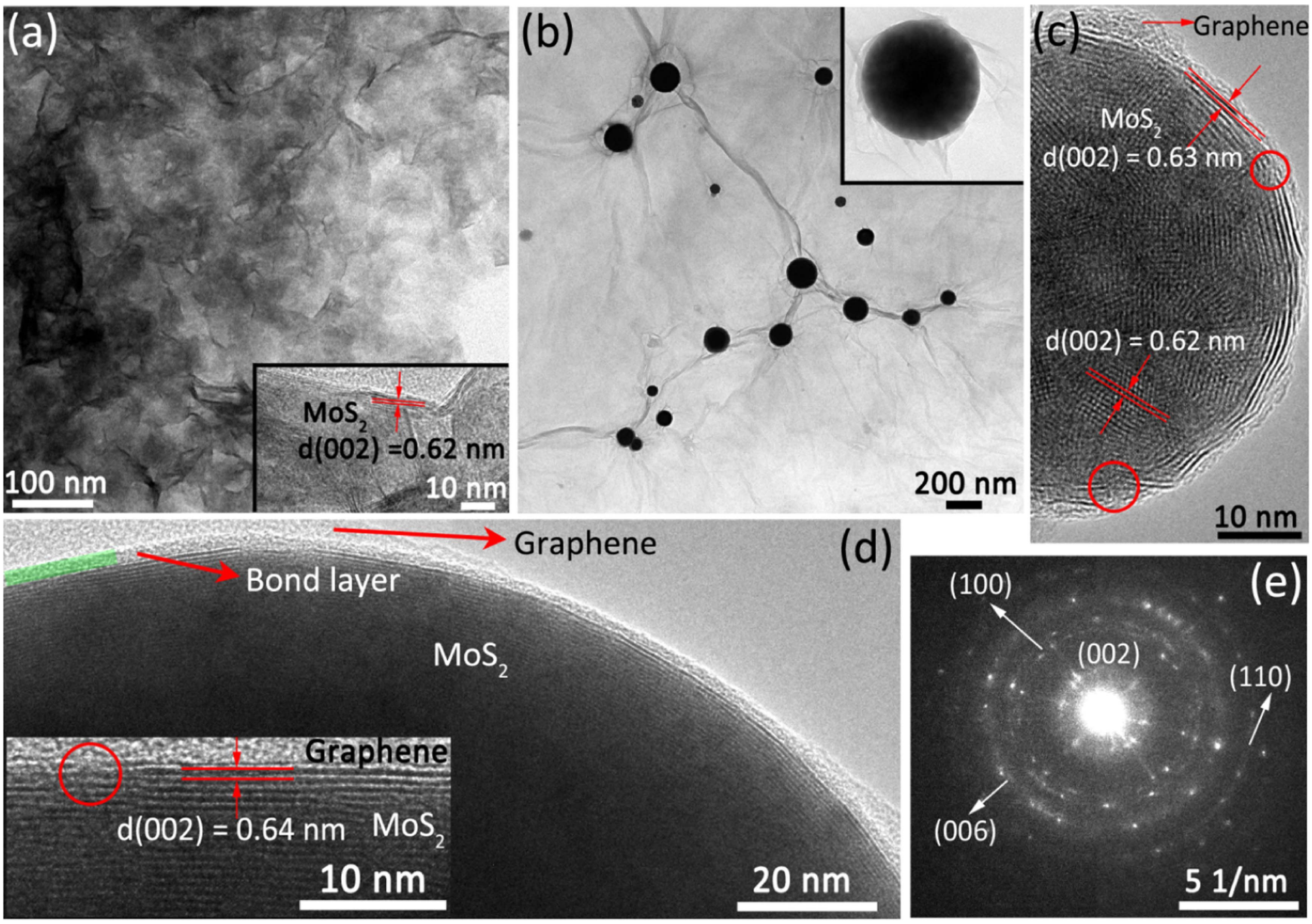

Figure 3. Microstructure analysis of the L-rGO/MoS_2 composite structure. TEM image of (a) raw GO/MoS_2 and (b) L-rGO/MoS_2 composite structure. (c)–(d) High-resolution TEM image of single MoS_2 spheres. (e) SAED pattern of the corresponding MoS_2 sphere.

from agglomeration and enables their good dispersion in the engine oil. The selected-area electron diffraction result reveals that the MoS_2 sub-microspheres are polycrystalline (figure 3(e)).

3.2. Formation mechanism of the L-rGO/MoS_2 composites

To systematically study the formation mechanism of the L-rGO/MoS_2 composite structures, we observed the shape evolution of the MoS_2 nanoflakes under laser irradiation for different times (figure S5). Laser irradiation of MoS_2 nanoflakes can create ultrahigh temperature and pressure within nanoseconds at a localized area [26, 27], which leads to bending and melting of the nanoflakes and subsequent evolvement into spherical particles under successive laser pulse heating and liquid quenching processes (figure 1). Due to the large specific surface area of GO nanosheets, significant optical absorption below 350 nm could result in a rapid rise in temperature and pressure, which induced the transformation of GO to graphene due to the photothermal reduction effect [28, 29], as shown in figure S3. This transformation process is reflected by the color evolution of GO solution from the original yellow golden to bronzing and eventually to black color. Moreover, the C=O absorption peak of GO at 304 nm disappeared after laser irradiation. The absorption of GO at 230 nm redshifts to 256 nm, induced by the $\pi \rightarrow \pi*$ transitions of extended aromatic C–C bonds after the KrF excimer laser irradiation [23, 29]. Overall, the deoxygenation of the GO nanosheets and the restoration of the sp^2 carbon sites in the graphene are confirmed.

The GO/MoS_2 hybrids possess layered structure with GO and MoS_2 nanoflakes stacking together due to their high specific surface energy [22]. Upon laser irradiation, the MoS_2 nanoflakes begin to bend and reshape into ultrasmooth spheres within the stacked graphene layers (figure 4). Meantime, GO is reduced to rGO. Eventually, L-rGO/MoS_2 composite structures with a large interlamellar spacing are obtained (figure 4(d)). More interestingly, owing to the really high temperature around the MoS_2 spheres, the graphene layer is formed around the MoS_2 spheres (figures 3 and S4), which can maintain MoS_2 spheres inside the graphene layers even under strong shear force when used as lubricant additives as discussed later.

3.3. Tribological properties of L-rGO/MoS_2 composites as oil additives

The dispersity of the L-rGO/MoS_2 composite structures in the bare engine oil is first investigated (figure 5(a)). No observable precipitations appeared even after 15 d in the engine oil,

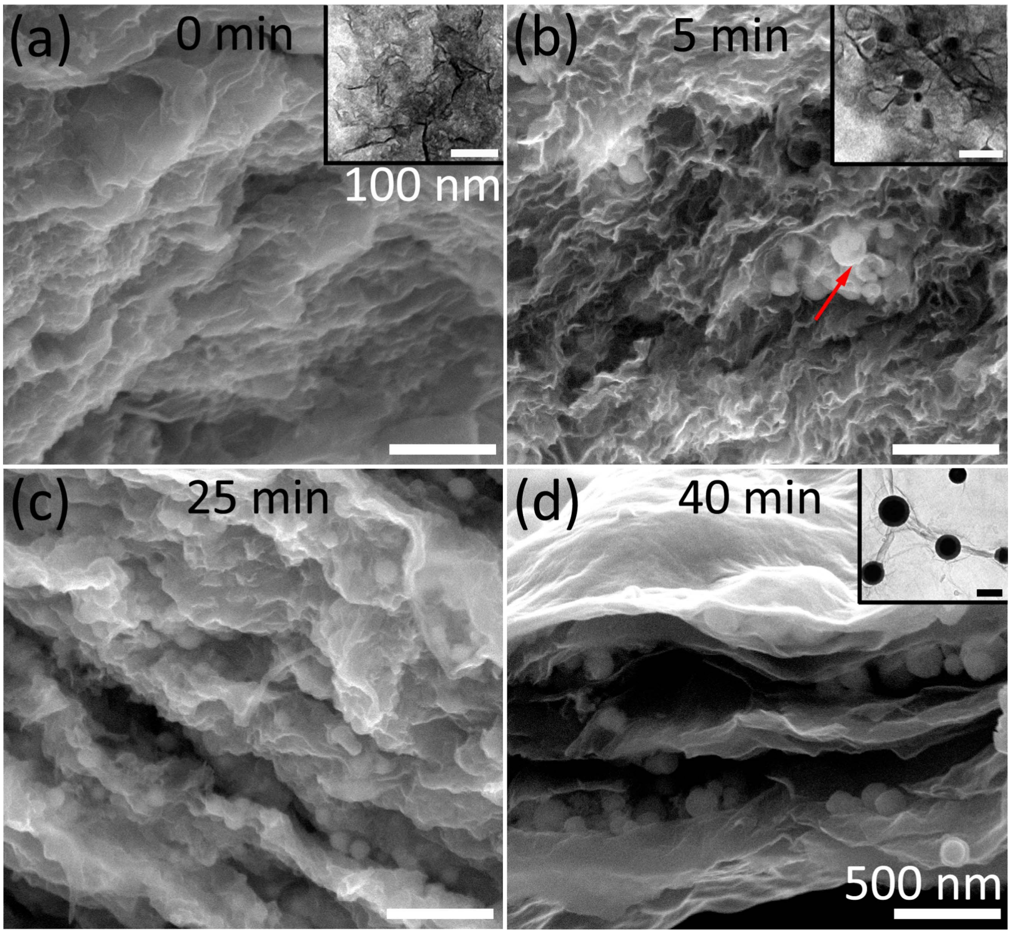

Figure 4. Formation process of the L-rGO/MoS_2 composite structure. Morphology evolution of the mixture of GO nanosheets and MoS_2 nanoflakes after laser irradiation for different times: (a) 0, (b) 5, (c) 25 and (d) 40 min. The laser fluency is 400 mJ pulse^{-1} cm^{-1}. Inset: corresponding TEM images. The red arrows show the early stage formation of spherical particles.

demonstrating that the laminated composite structures could stably disperse in the engine oil. In contrast, obvious precipitations emerged in the solution composed of GO/MoS_2 after only 1 d. These results are consistent with the Zeta potential and the morphological measurements (figures S6 and S7). The absolute value of the Zeta potential of the solution composed of 0D/2D L-rGO/MoS_2 composite structures is much higher than that of the solution composed of GO/MoS_2. Due to the flat, disk-like shape and high specific surface energy of MoS_2 flakes and GO nanosheets, they are prone to aggregating together. These aggregates tend to precipitate in the engine oil. Oppositely, the crumpled surface of the L-rGO/MoS_2 composite structures prevents them from attacking each other and makes them stably disperse in engine oil [6, 30].

The tribological properties of the L-rGO/MoS_2 composites as engine oil additives at a concentration of 0.2 wt% (figure S8) were evaluated by a four-ball tribology tester (figure 5(b)). To compare, the same tribology tests were performed on the pure engine oil and the engine oil containing rGO nanosheets, MoS_2 nanoflakes, laser irradiation-created perfectly spherical MoS_2 particles, and GO/MoS_2 hybrids, respectively. During the first 5 min, the coefficients of friction (referred as COF) increase for all of the lubricants, which is because the contact between the balls transformed from point contact to surface contact (figure 5(c)). All of the additives can reduce the COF after the friction coefficient is stabilized. Graphene additives can reduce the COF by about 6% when compared to that of the pure engine oil. The COF of MoS_2 nanoflake additives is on average comparable to that of the graphene additives, but increases gradually. By introducing GO/MoS_2 into the engine oil, the COF is reduced to a larger extent than only introducing one of the two. The laser irradiation produced ideally MoS_2 spheres as lubricant additives can effectively reduce the COF by ~17% when compared with that of the pure engine oil. This is because the ultrasmooth spherical particles can effectively turn sliding friction into the rolling friction [31, 32]. Strikingly, the L-rGO/MoS_2 composite structures can reduce the COF by ~25% when compared with that of the pure engine oil (figures 5(c) and (e)). Notably, the friction coefficient of the engine oil composed of 0D/2D L-rGO/MoS_2 composite structures fluctuates very slightly (<~2%) and does not show obvious increase during the measurement. In contrast, the friction coefficient of pristine engine oil and engine oil with other four additives all shows obvious fluctuations (>10%) (figure 5(b)). Additionally, the friction coefficient of the 0D/2D L-rGO/MoS_2 composites does not change too much even working under 75 °C (figure 5(e)). In contrast, the pure engine

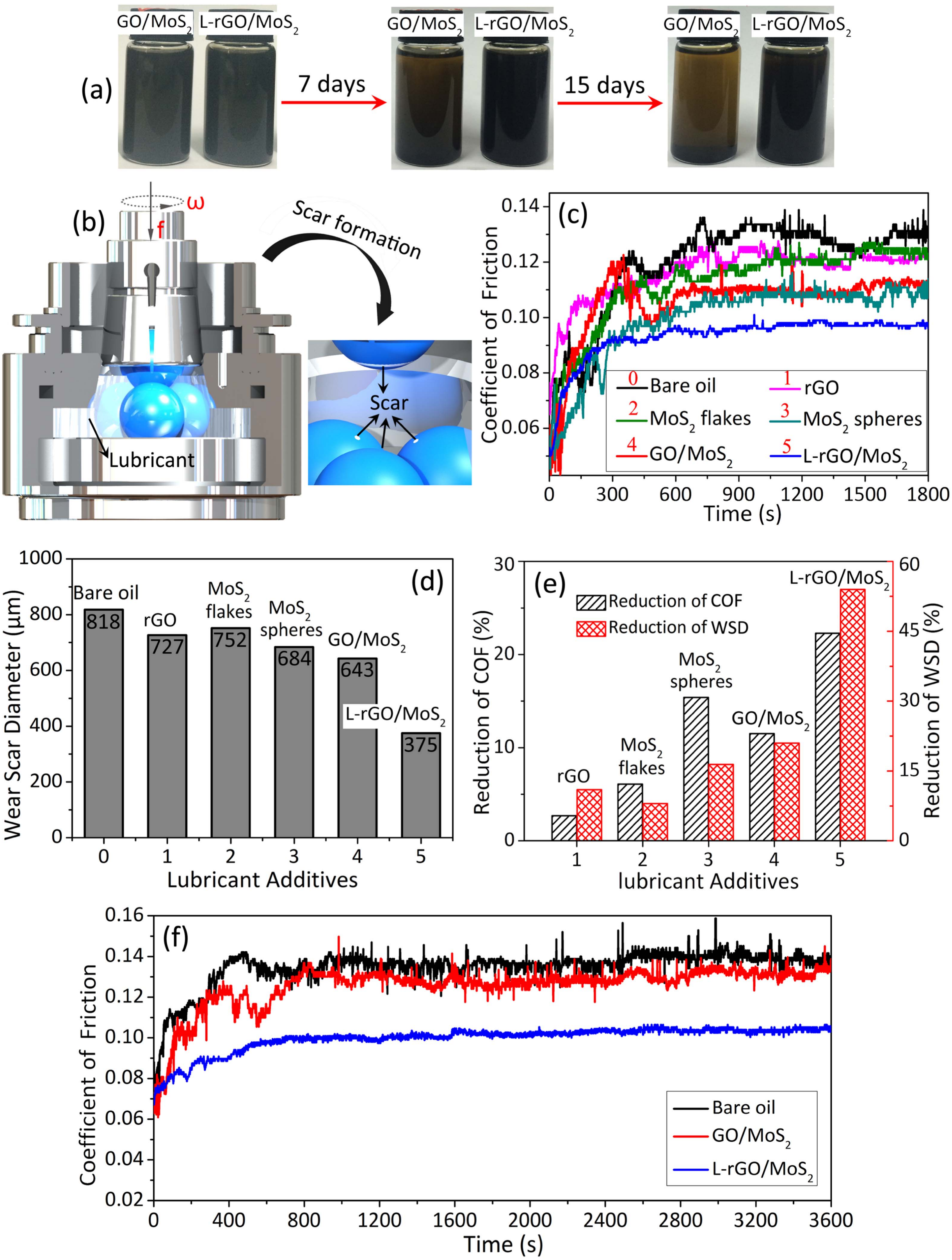

Figure 5. Friction reduction and anti-wear properties. (a) Dispersion properties of raw GO/MoS_2 hybrids and L-rGO/MoS_2 composites. (b) Schematic of the four-ball tribology tester for friction coefficient and wear scar measurements. (c) COF and (d) WSD of the engine oil with different additives (0.2 wt%) after running for 30 min at room temperature. (e) The corresponding reduction percentage of average COF and WSD compared with those of the bare engine oil. (f) COF of the bare oil and the oil contained GO/MoS_2 and L-rGO/MoS_2 composite structure for 60 min at 75 °C.

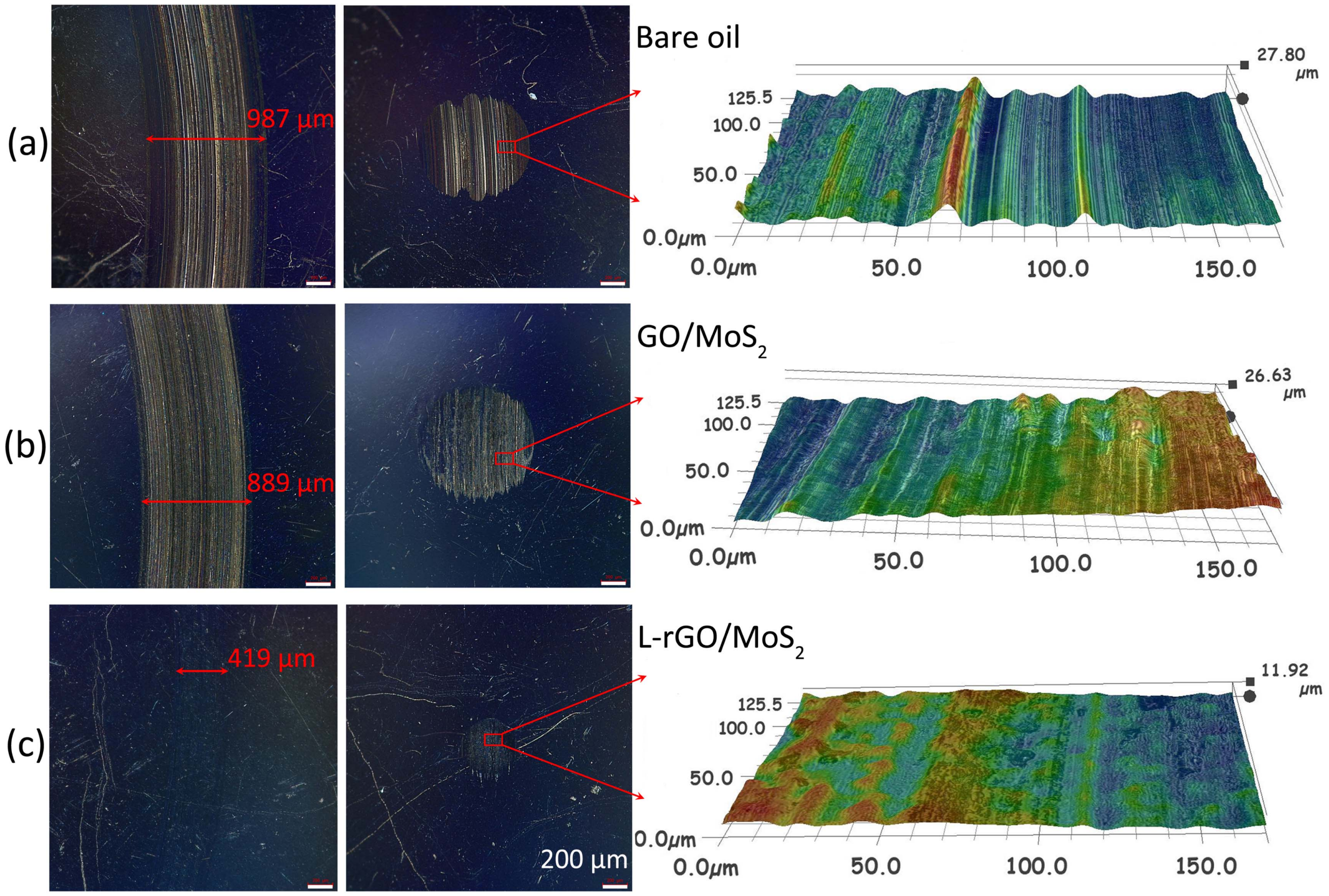

Figure 6. Optical images (left column) and the corresponding 3D profile images (right column) of the wear surfaces lubricated sliding with (a) bare oil, (b) raw GO/MoS_2 hybrids, and (c) L-rGO/MoS_2 composites for 60 min at 75 °C.

oil and the oil contained GO/MoS_2 increases prominently at high temperatures, owing to the rupture of boundary film at adhesion point.

Desirable lubricant additives should not only be able to reduce friction, but also have good anti-wear properties since serious wear will cause mechanical failure of the engine [33–36]. The anti-wear property is usually evaluated by the WSD on moving balls. All of the lubricant additives can reduce the WSD (figures 5(d), (e)). In order to clearly observe the wear scar, the top rotating ball and one stationary ball lubricated sliding with bare oil, raw GO/MoS_2 hybrids, and L-rGO/MoS_2 composites for 60 min at 75 °C, were characterized by a LSCM, as shown in figure 6. Raw GO/MoS_2 additives reduce the WSD on stationary ball by only ~10% when compared to that of the pure engine oil. In particular, introducing the L-rGO/MoS_2 composite structures into the engine oil, the WSD on stationary ball decreases from 987 to 419 μm (~58% reduction). The 3D maps of the wear area on stationary balls indicate the wear tracks are very shallow and small. The absence of deep and wide wear tracks can prevent the formation of large debris that can inflict severe abrasive wear [37, 38]. Therefore, no obvious wear tracks on the rotating ball are produced and the WSD decreases by about 58%, which outperforms most of the previously reported lubricant oil additives under such a high-load and rotation speed (table S1). Overall, the 0D/2D L-rGO/MoS_2 composite structures are excellent lubricant additives with outstanding dispersion stability in lubricating oil and friction reduction and excellent anti-wear tribological properties.

3.4. Working mechanism in friction reduction and anti-wear processes

To clarify the lubricating mechanism of the L-rGO/MoS_2 composite structure as lubricant additives, we analyzed the wear area composition after the tribology test with the Raman spectrometer and energy-dispersive x-ray spectrometer (EDS). In light of the discontinuity of tribofilm after repeated cleaning by petroleum ether, acetone and alcohol, we performed Raman intensity mapping over a larger area (100 × 75 μm) in the wear scar (the red box), as shown in figure 7(a). Raman intensity mapping images of the graphene G mode and the MoS_2 A_{1g} mode indicate the transfer of graphene and MoS_2 to metal friction surface. The existence of Mo and S elements (figure 7(b)) on the wear area also indicates the formation of tribofilm on wear surfaces by the 0D/2D L-rGO/MoS_2 composite structures. Due to the large specific area of graphene, the laminated composite structure has a great chance to be transferred into the metal-to-metal contact surface area during the ball movement to prevent metal-to-metal direct contact, acting as a spacer to prevent the scar formation [22, 39]. More importantly, the quasi-fullerene-like MoS_2 spheres between the graphene layers can change

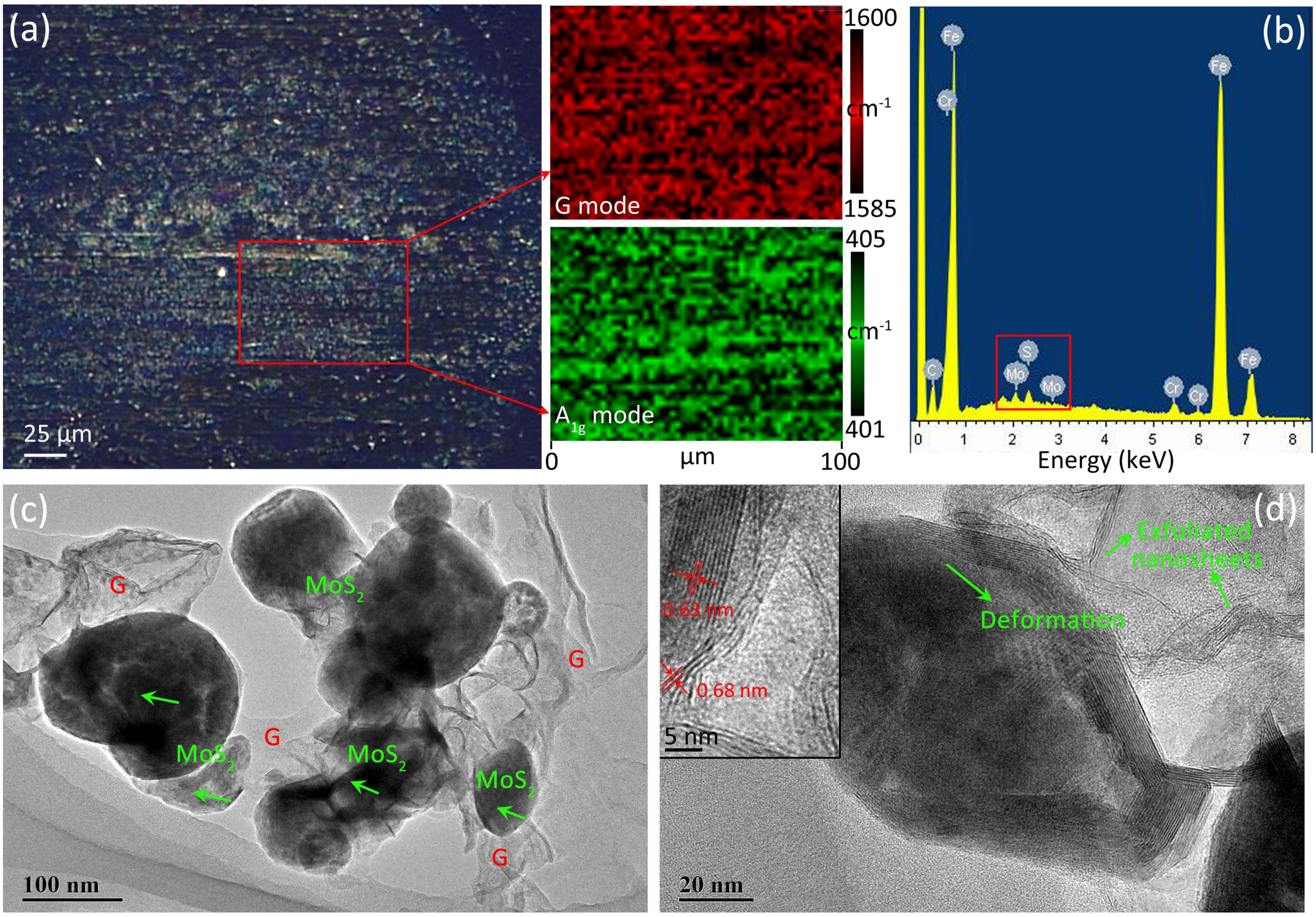

Figure 7. Working mechanism of the L-rGO/MoS_2 composites regarding friction reduction and anti-wear. (a) Raman intensity mapping images of graphene with the G mode (red) and MoS_2 with the A_{1g} mode (green). (b) EDS of the wear area lubricated by engine oil composed of L-rGO/MoS_2 composites for 60 min under 75 °C. (c) and (d) TEM images show the morphology and microstructure of L-rGO/MoS_2 composite structure after the tribology test. The deformation of MoS_2 nanospheres and exfoliation of nanosheets are observed.

sliding friction into rolling friction under the strong shear force caused by the moving balls, making the 0D/2D L-rGO/MoS_2 composite structures analogous to micro-bearings to greatly reduce the friction [31]. So, the micro-bearing spheres can be deformed or even exfoliated under high-load shear force, as shown in figures 7(c), (d). Then these exfoliated flake-like MoS_2 nanosheets as additives still protect the steel surfaces.

In addition, the raw MoS_2 nanoflakes are of highly chemical activity as there are many chemical dangling bonds at the edge sites. So, MoS_2 nanoflakes are easily oxidized to MoO_x, which is generally considered as a main reason for the invalidation of MoS_2 lubricants because of the damage of layered structure [31, 33]. The quasi-fullerene-like MoS_2 spheres are rare with dangling bonds, as well as they are protected by the circumjacent graphene layers, allowing L-rGO/MoS_2 composites to be used under high temperatures without being oxidized (figures 8 and S9).

4. Conclusions

Comprehensively considering the working mechanism of inorganic particles as lubricant additives, we construct a novel laminated lubricant additives that can combine the advantages of 0D and 2D structured lubricant additives. A simple one-step method is developed to prepare the L-rGO/MoS_2 composite structure by laser irradiation of a dispersion composed of MoS_2 nanoflakes and GO nanosheets in ambient conditions. The high temperature and pressure created by the laser irradiation can reshape the MoS_2 nanoflakes into perfectly spherical particles with a quasi-fullerene-like structure and meantime reduce the GO into rGO. The laminated composite structures are composed of ultrasmooth MoS_2 sub-micro-spheres embedded within multiple layers of graphene. The spherical MoS_2 particles can change sliding friction into rolling friction under strong shear force to effectively reduce the friction. At the same time, the 2D graphene layers as lubricant additives can protect the metal contacting surfaces from being scratched, significantly enhancing the anti-wear performance of the lubricant. Overall, the 0D/2D L-rGO/MoS_2 composites have outstanding tribological properties even under high working temperatures when used as lubricant additives, better than conventional nanoparticles and 2D materials. These characteristics endow them with great application potentials as high-performance practical lubricant additives.

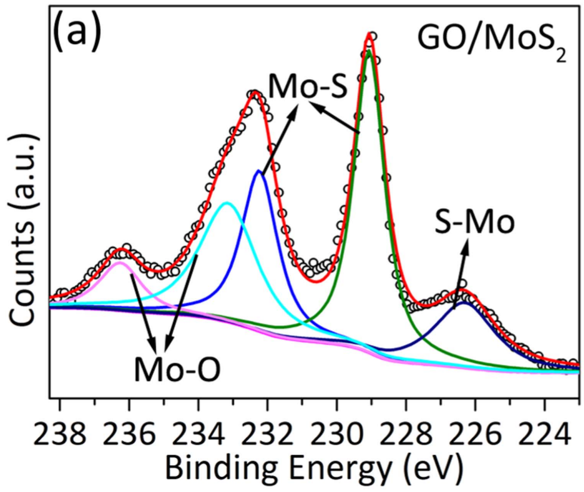

Figure 8. XPS spectra of (a) raw GO/MoS_2 hybrids and (b) L-rGO/MoS_2 composites used as lubricant additives after tribology test for 60 min under 75 °C.

Acknowledgments

This work was supported by NSFC (51472110, 51671094, and 51702283) and NSF of Shandong Province (ZR2016BM25). BQ Cao acknowledges the Taishan Scholar Professorship tenured at University of Jinan SY acknowledges support from the 'National 1000 Young Talent Program' and 'Zhejiang University 100 Talent Program'.

ORCID iDs

Shikuan Yang https://orcid.org/0000-0001-6662-3057

References

[1] Altavilla C, Sarno M, Ciambelli P, Senatore A and Petrone V 2013 New 'chimie douce'approach to the synthesis of hybrid nanosheets of MoS_2 on CNT and their anti-friction and anti-wear properties *Nanotechnology* **24** 125601
[2] Chen X, Zhang C, Kato T, Yang X, Wu S, Wang R, Nosaka M and Luo J 2017 Evolution of tribo-induced interfacial nanostructures governing superlubricity in a-C:H and a-C:H:Si films *Nat. Commun.* **8** 1675
[3] Gigli L, Manini N, Benassi A, Tosatti E, Vanossi A and Guerra R 2017 Graphene nanoribbons on gold: understanding superlubricity and edge effects *2D Mater.* **4** 045003
[4] Erdemir A, Ramirez G, Eryilmaz O L, Narayanan B, Liao Y, Kamath G and Sankaranarayanan S K 2016 Carbon-based tribofilms from lubricating oils *Nature* **536** 67–71
[5] Wang X B and Liu W M 2013 Nanoparticle-based lubricant additives *Encyclopedia of Tribology* (New York: Springer) pp 2369–76
[6] Spear J C, Ewers B W and Batteas J D 2015 2D-nanomaterials for controlling friction and wear at interfaces *Nano Today* **10** 301–14
[7] Dou X, Koltonow A R, He X, Jang H D, Wang Q, Chung Y W and Huang J 2016 Self-dispersed crumpled graphene balls in oil for friction and wear reduction *Proc. Natl Acad. Sci. USA* **113** 1528–33
[8] Lahouij I, Vacher B, Martin J M and Dassenoy F 2012 IF-MoS_2 based lubricants: influence of size, shape and crystal structure *Wear* **296** 558–67
[9] Song X, Qiu Z, Yang X, Gong H, Zheng S, Cao B, Wang H, Möhwald H and Shchukin D 2014 Submicron-lubricant based on crystallized Fe_3O_4 spheres for enhanced tribology performance *Chem. Mater.* **26** 5113–9
[10] Zou T Z, Tu J P, Huang H D, Lai D M, Zhang L L and He D N 2006 Preparation and tribological properties of inorganic fullerene-like MoS_2 *Adv. Eng. Mater.* **8** 289–93
[11] Rapoport L, Fleischer N and Tenne R 2005 Applications of WS_2 (MoS_2) inorganic nanotubes and fullerene-like nanoparticles for solid lubrication and for structural nanocomposites *J. Mater. Chem.* **15** 1782–8
[12] Luo T, Wang P, Qiu Z, Yang S, Zen H and Cao B 2016 Smooth and solid WS_2 sub-microspheres grown by a new laser fragmentation and reshaping process with enhanced tribological properties *Chem. Commun.* **52** 10147–50
[13] Wu Y, Zeng X, Ren T, de Vries E and van der Heide E 2017 The emulsifying and tribological properties of modified graphene oxide in oil-in-water emulsion *Tribol. Int.* **105** 304–16
[14] Zhang W *et al* 2011 Tribological properties of oleic acid-modified graphene as lubricant oil additives *J. Phys. D: Appl. Phys.* **44** 205303
[15] Sarno M, Senatore A, Cirillo C, Petrone V and Ciambelli P 2014 Oil lubricant tribological behaviour improvement through dispersion of few layer graphene oxide *J. Nanosci. Nanotechnol.* **14** 4960–8
[16] Wu Y, Li H, Ji L, Liu L, Ye Y, Chen J and Zhou H 2013 Structure, mechanical, and tribological properties of MoS_2/a-C: H composite films *Tribol. Lett.* **52** 371–80
[17] Kim S Y, Kwak J, Kim J H, Lee J U, Jo Y, Kim S Y, Cheong H, Lee Z and Kwon S Y 2016 Substantial improvements of long-term stability in encapsulation-free WS_2 using highly interacting graphene substrate *2D Mater.* **4** 011007
[18] Silbert L E 2010 Jamming of frictional spheres and random loose packing *Soft Matter* **6** 2918–24
[19] Zhou X, Wu D, Shi H, Fu X, Hu Z, Wang X and Yan F 2007 Study on the tribological properties of surfactant-modified MoS_2 micrometer spheres as an additive in liquid paraffin *Tribol. Int.* **40** 863–8
[20] Rabaso P, Dassenoy F, Ville F, Diaby M, Vacher B, Le Mogne T, Belin M and Cavoret J 2014 An investigation on the reduced ability of IF-MoS_2 nanoparticles to reduce

friction and wear in the presence of dispersants *Tribol. Lett.* **55** 503–16
[21] Rosentsveig R, Margolin A, Gorodnev A, Popovitz-Biro R, Feldman Y, Rapoport L, Novema Y, Naveh G and Tenne R 2009 Synthesis of fullerene-like MoS_2 nanoparticles and their tribological behavior *J. Mater. Chem.* **19** 4368–74
[22] Abdelsayed V, Moussa S, Hassan H M, Aluri H S, Collinson M M and El-Shall M S 2012 Photothermal deoxygenation of graphite oxide with laser excitation in solution and graphene-aided increase in water temperature *J. Phys. Chem. Lett.* **1** 2804–9
[23] Lamberti A, Serrapede M, Ferraro G, Fontana M, Perrucci F, Bianco S, Choilerio A and Bocchini S 2017 All-SPEEK flexible supercapacitor exploiting laser-induced graphenization *2D Mater.* **4** 035012
[24] Hou S, Birowosuto M D, Umar S, Ange A M, Tay R Y, Philippe C, Tay B K, Wang H and Teo E H T 2018 Localized emission from laser-irradiated defects in two-dimensional hexagonal boron nitride *2D Mater.* **5** 015010
[25] Yang G W 2007 Laser ablation in liquids: applications in the synthesis of nanocrystals *Prog. Mater. Sci.* **52** 648–98
[26] Wang H, Koshizaki N, Li L, Jia L, Kawaguchi K, Li X, Pyatenko A, Swiatkowska-Warkocka Z, Bando Y and Golberg D 2011 Size-tailored ZnO submicrometer spheres: bottom-up construction, size-related optical extinction, and selective aniline trapping *Adv. Mater.* **23** 1865
[27] El-Kady M F, Strong V, Dubin S and Kaner R B 2012 Laser scribing of high-performance and flexible graphene-based electrochemical capacitors *Science* **335** 1326–30
[28] Zedan A F, Moussa S, Terner J, Atkinson G and El-Shall M S 2012 Ultrasmall gold nanoparticles anchored to graphene and enhanced photothermal effects by laser irradiation of gold nanostructures in graphene oxide solutions *ACS Nano* **7** 627–36
[29] Hummers W S Jr and Offeman R E 1958 Preparation of graphitic oxide *J. Am. Chem. Soc.* **80** 1339
[30] Paredes J I, Villar-Rodil S, Martínez-Alonso A and Tascon J M D 2008 Graphene oxide dispersions in organic solvents *Langmuir* **24** 10560–4
[31] Hu K, Hu X, Xu Y, Huang F and Liu J 2010 The effect of morphology on the tribological properties of MoS_2 in liquid paraffin *Tribol. Lett.* **40** 155–65
[32] Rapoport L, Feldman Y, Homyonfer M, Cohen H, Sloan J, Hutchison J L and Tenne R 1999 Inorganic fullerene-like material as additives to lubricants: structure-function relationship *Wear* **225** 975–82
[33] Manimunda P, Nakanishi Y, Jaques Y M, Susarla S, Woellner C F, Bhowmick S, Asif S A S, Galvão D S, Tiwary C S and Ajayan P M 2017 Nanoscale deformation and friction characteristics of atomically thin WSe_2 and heterostructure using nanoscratch and raman spectroscopy *2D Mater.* **4** 045005
[34] Gallagher P *et al* 2016 Switchable friction enabled by nanoscale self-assembly on graphene *Nat. Commun.* **7** 10745
[35] Liechti K M 2015 Understanding friction in layered materials *Science* **348** 632–3
[36] Li S, Li Q, Carpick R W, Gumbsch P, Liu X Z, Ding X, Sun J and Li J 2016 The evolving quality of frictional contact with graphene *Nature* **539** 541–5
[37] Ronen A and Malkin S 1981 Wear mechanisms of statically loaded hydrodynamic bearings by contaminant abrasive particles *Wear* **68** 371–89
[38] Meng Y, Su F and Chen Y 2016 Supercritical fluid synthesis and tribological applications of silver nanoparticle-decorated graphene in engine oil nanofluid *Sci. Rep.* **6** 31246
[39] Koshy C P, Rajendrakumar P K and Thottackkad M V 2015 Evaluation of the tribological and thermo-physical properties of coconut oil added with MoS_2 nanoparticles at elevated temperatures *Wear* **330** 288–308